ACS Energy LETTERS

http://pubs.acs.org/journal/aelccp

LETTER

Mechanism of Tin Oxidation and Stabilization by Lead Substitution in Tin Halide Perovskites

Tomas Leijtens,*[,†,∥] Rohit Prasanna,[†,∥] Aryeh Gold-Parker,[‡,§] Michael F. Toney,[§] and Michael D. McGehee*[,†]

[†]Department of Materials Science, Stanford University, 476 Lomita Mall, Stanford, California 94305, United States

[‡]Department of Chemistry, Stanford University, Stanford, California 94305, United States

[§]Stanford Synchrotron Radiation Lightsource, SLAC National Accelerator Laboratory, Menlo Park, California 94025, United States

Supporting Information

ABSTRACT: **The recent development of efficient binary tin- and lead-based metal halide perovskite solar cells has enabled the development of all-perovskite tandem solar cells, which offer a unique opportunity to deliver high performance at low cost. Tin halide perovskites, however, are prone to oxidation, where the Sn^{2+} cations oxidize to Sn^{4+} upon air exposure. Here, we identify reaction products and elucidate the oxidation mechanism of both $ASnI_3$ and $ASn_{0.5}Pb_{0.5}I_3$ (where A can be made of methylammonium, formamidinium, cesium, or a combination of these) perovskites and find that substituting lead onto the B site fundamentally changes the oxidation mechanism of tin-based metal halide perovskites to make them more stable than would be expected by simply considering the decrease in tin content. This work provides guidelines for developing stable small band gap materials that could be used in all-perovskite tandems.**

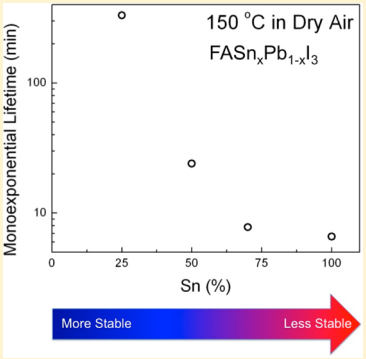

All-perovskite tandem solar cells offer a great opportunity for reducing the cost and raising the efficiency of solar cells.[1−5] Such multijunction perovskite solar cells rely heavily on the development of efficient and stable low-band gap (1.1−1.3 eV) perovskite absorbers. Recently, we and other research groups have demonstrated perovskites with band gaps approaching 1.2 eV by mixing Sn and Pb on the B site of the ABX_3 perovskite structure.[1,5,6] Indeed, we succeeded in making low band gap devices with 14.8% PCE and used these in a monolithic two-terminal tandem with 17.0% PCE and a mechanically stacked tandem with 20.3% PCE. Yan et al. more recently developed $MA_{0.4}FA_{0.6}Sn_{0.6}Pb_{0.4}I_3$ (MA = methylammonium = CH_3NH_3, FA = formamidinium = $HC(NH_2)_2$) perovskite solar cells with small band gaps (∼1.25 eV) and efficiencies of 17.1% PCE, which translated to a 21% mechanically stacked all-perovskite four-terminal tandem[2] while Jen et al. used $MASn_{0.5}Pb_{0.5}I_3$ to make 18.5% efficient monolithic tandems with high voltages.[7] While device performances are promising, Sn^{2+}-based perovskites are notoriously prone to oxidation,[8−11] and the stability of the small band gap solar cells is thus an important subject for research. Early reports by Noel et al.[9] and Kanatzidis et al.[12] proposed that the Sn^{2+} in $MASnI_3$ perovskites is oxidized to Sn^{4+}, resulting in Sn^{2+} vacancies that are recombination centers.[9,12] The proposed mechanism was that Sn^{2+} to Sn^{4+} oxidation results in SnI_4 gas evolution and associated Sn^{2+} and I^- vacancies. Numerous reports have since demonstrated that the crystalline structure, absorption profile, and device performance deteriorate rapidly (minutes) in air,[1,8−13] so that the stability of tin-based perovskites can be considered to be the largest hurdle facing the development of all-perovskite tandem solar cells based on tin containing small band gap perovskites. In addition, understanding has thus far been lacking, preventing a rational approach to controlling the oxidation in tin-based perovskites. Surprisingly, we and others have recently found that incorporating Pb into Sn-based perovskite solar cells dramatically enhances their air stability,[1,5] but a mechanistic understanding has thus far not been obtained, limiting possible improvements in stability of all perovskite tandems.

Here, we elucidate the degradation mechanisms of tin halide and mixed tin−lead halide perovskites. Using in situ X-ray diffraction measurements (XRD), we find that the Sn:Pb ratio plays a large role in determining the degradation kinetics of the materials in air, with higher Pb contents resulting in slower oxidation kinetics. We go on to use thermogravimetric analysis (TGA) and ultraviolet (UV)−visible absorption spectroscopy to identify the degradation pathways and end products of tin halides and tin halide perovskites with various lead contents. Our findings suggest that oxidation of pure tin halide and tin halide perovskite materials occurs via a cooperative mechanism involving multiple adjacent Sn^{2+} ions to form SnO_2 and SnI_4. Mixed Sn−Pb containing compounds oxidize much more

Received: July 21, 2017
Accepted: August 24, 2017
Published: August 24, 2017

DOI: 10.1021/acsenergylett.7b00636
ACS Energy Lett. 2017, 2, 2159−2165

slowly, more so than can be explained simply by considering that there is less tin to oxidize. Here, the reaction mechanism is altered and the main products are I_2, SnO_2, and PbI_2. Because there is a high probability that a Sn^{2+} that is being oxidized will have Pb^{2+} in adjacent octahedra, which are far more difficult to oxidize, the cooperative mechanism that facilitates oxidation of pure tin halide perovskites becomes less favorable.

To quantify the oxidation kinetics of $FASn_xPb_{1-x}I_3$ films, we heated films (~300 nm) with varying Sn content in dry air and monitored their X-ray diffraction during the degradation. We employ the film deposition method described in our previous work, which yields similar film morphology and grain sizes for the full range of Sn:Pb rations.[1] The XRD patterns are plotted in Figure S1 and demonstrate that the materials undergo rapid degradation upon heating in dry air, while the XRD spectra are unchanged at 85 °C in He atmosphere (Figure S2). We are thus confident that the observed degradation is the result of oxidation rather than any thermal effect. We observe that the peak intensities diminish evenly across the pattern, indicating no change in orientation or structure of the materials during oxidation. We also do not find evidence for any crystalline degradation products. Instead, as the materials oxidize, we observe only a decrease in scattering from crystalline perovskite. Integrating the cubic (100) peak intensities and plotting them over time, we can quantify the degradation kinetics as a function of Sn content and temperature. Figure 1a displays the degradation kinetics for $FASnI_3$ and $FASn_{0.5}Pb_{0.5}I_3$ at 85 °C in dry air and shows that incorporating 50% Pb into $FASnI_3$ can dramatically enhance its air stability. In Figure S3, we plot degradation kinetics for several temperatures and find that both pure Sn and Sn−Pb compounds degrade much more readily at higher temperatures, consistent with the oxidation being a thermally activated process. We also plot the degradation kinetics of a wider range of Sn:Pb ratios at 150 °C in Figure S4 and find that the compounds with the highest lead content are the most stable. The monoexpontial lifetimes (from fitting the first 50% of the decays) for these are plotted in Figure 1b, demonstrating a strong and nonlinear dependence on tin content.

This set of measurements demonstrates that tin-based perovskite materials suffer from rapid oxidation that is accelerated by heat and is slowed as lead is incorporated into the material. Compositions with 50% Sn or less are far more stable than the pure tin compounds and more so than could be explained by simply considering the fact that there is less Sn to be oxidized. Indeed, the lifetimes as a function of Sn content (Figure 1b) appear to fall into two regimes: those with high tin contents and those with ~50% or less. This suggests that as the Pb content is increased to ~50% or less, the oxidation mechanism could be fundamentally changed. Compounds containing only 25% Sn (Figures 1b and S4) offer significantly improved resistance to oxidation and can deliver high performances[5] at moderately low band gaps (~1.35 eV). A 1.35 eV band gap is suitable for single-junction solar cells, so this material may become an attractive efficient and stable compound for single-junction perovskite solar cells. Here, however, we focus our attention on compounds containing 50% Pb because those have the lowest band gaps and are currently the most suitable for multijunction applications.[1,2]

We prepared a simple alloy of SnI_2 and PbI_2: $Sn_{0.5}Pb_{0.5}I_2$ (or $SnPbI_4$) to use as a model system so that we can ignore the effects of the A site cation. Films of this material exhibit just one phase in XRD, the hexagonal phase shared by PbI_2 and the

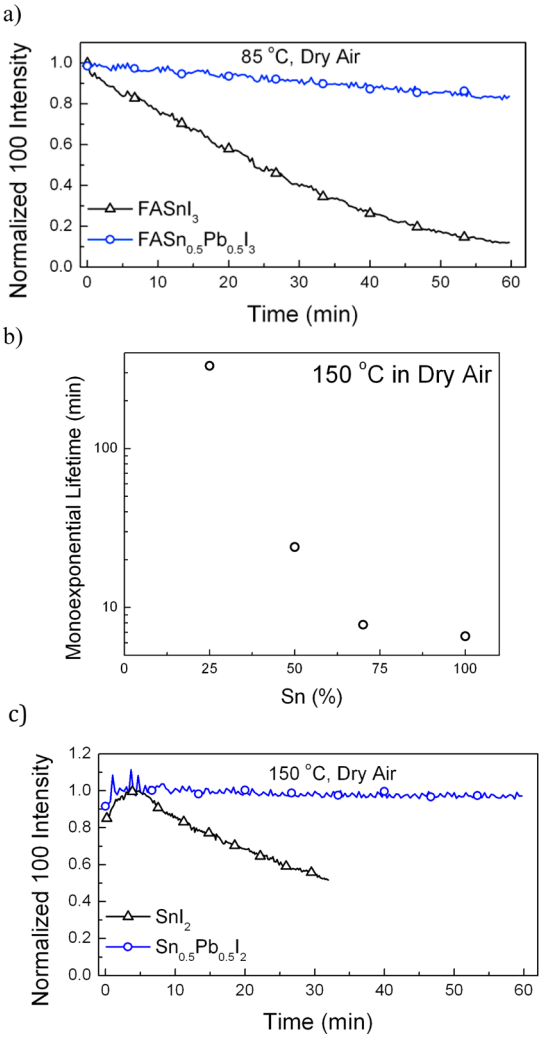

Figure 1. Normalized cubic (100) XRD peak intensity as a function of time in dry air. We compare the decay in peak intensity as a function of time in dry air for $FASn_xPb_{1-x}I_3$ with x = 0.5 and 1 at 85 °C in panel a. The monoexponential lifetime of 25, 50, 70, and 100% Sn perovskite compounds at 150 °C in dry air is plotted in panel b. The degradation of $SnPbI_4$ and SnI_2 in dry air is monitored at 150 °C (c).

high-temperature phase of SnI_2[14] (see Figure S5). When exposed to dry air at 150 °C, the alloy exhibits improved stability over the SnI_2 films, as shown in Figure 1c. In fact, it does not degrade at all over the course of 1 h in air at 150 °C. This not only gives us insights into the enhanced stability of Sn:Pb mixed perovskite compounds but also offers a route to improving the shelf life and ease of handling of tin halide precursors for tin-based perovskite solar cells.

There are two most likely oxidation pathways for SnI_2. In the first, all of the SnI_2 is simply oxidized to SnO_2 and the iodide evolves as I_2[15] (Table 1, reaction scheme 2). This requires the oxidation of both the tin and iodide species and also requires many Sn−I bonds to be broken. The other mechanism produces equimolar SnI_4 and SnO_2[15] (Table 1, reaction scheme 1). Here, fewer Sn−I bonds are broken: in reaction scheme 1, all four Sn−I bonds are broken, as opposed to just two in reaction scheme 2.

Suzuki et al.[15−17] previously used thermogravimetric analysis in air and N_2 to identify the oxidation reaction mechanism and

DOI: 10.1021/acsenergylett.7b00636
ACS Energy Lett. 2017, 2, 2159−2165

Table 1. Possible Steps in Oxidation Mechanisms and Associated Predicted Mass Losses[a]

	Mass Loss(%)	Final Mass(%)
SnI_2		
(1) $2SnI_2 + O_2 \Rightarrow SnO_2 + SnI_4(g)$	*79.7*	*20.3*
(2) $SnI_2 + O_2 \Rightarrow SnO_2 + I_2(g)$	59.5	40.5
Measured	**78.0 (±.1)**	**22.0(±.1)**
$FASnI_3$		
(3a) $2FASnI_3 + O_2 \Rightarrow 2FAI(s) + SnO_2 + SnI_4(g)$	*54.5*	*45.5*
(3b) $\Rightarrow 2FAI(g) + SnO_2 + SnI_4(g)$	*86.1*	*13.9*
(4a) $FaSnI_3 + O_2 \Rightarrow FAI(s) + SnO_2 + I_2(g)$	40.6	59.4
(4b) $\Rightarrow FAI(g) + SnO_2 + I_2(g)$	72.2	27.8
Measured (±2, ±0.1)	**63, 85.2**	**37, 14.8**

[a]The mechanisms in blue are those that agree with our measured experimental data (boldface). In a multistep reaction, the steps are tabulated as cumulative mass losses associated with the first and then second steps, defined by considering reductions in the slope of the mass versus temperature (Supporting Information).

products of SnI_2 in air. They demonstrated via TGA, XRD, and DSC measurements that SnI_2 degrades to equimolar SnI_4 and SnO_2 when heated or illuminated in air. SnI_4 sublimes at low temperatures (~100−150 °C), so its formation resulted in large mass loss from the sample as SnI_2 was oxidized. They found that the oxidation mechanism was the same regardless of whether it was accelerated by light or heat. In TGA analysis, one tabulates the expected mass losses for the possible reaction pathways and compares these to the experimentally measured ones. The two most likely oxidation routes for SnI_2 are described together with their mass losses in Table 1. Simply put, the oxidation of tin halide compounds can proceed via two general mechanisms: one by which all of the Sn−I bonds are broken and the products are SnO_2 and I_2, and one by which fewer Sn−I bonds are broken and SnI_4 and SnO_2 are the degradation products. TGA can distinguish between the two because high mass losses must imply the formation and evolution of SnI_4 as this involves the mass loss of both iodine and tin rather than just iodine.

We performed TGA on SnI_2 in both air and N_2 atmospheres (see Figure 2a) and observe that the mass loss in air occurs at far lower temperatures than that in N_2, confirming that the oxidation reaction induces a significant mass loss. Following the procedure from Suzuki et al.,[15] we then can compare the measured final mass (denoted as "Measured" in Table 1) to those predicted from the possible reaction schemes described above and detailed in Table 1. We conclude, as did Suzuki et al., that the primary reaction pathway must involve sublimation of SnI_4 for the mass loss to be as high as we measured it to be (78%). We denote the most likely reaction pathways in Table 1 by italicizing them and presenting them in blue. We also point out that there is no further mass loss after 350 °C for the SnI_2 compound in air, which means that the remnant material must have a sublimation temperature that is much higher than that the starting materials, consistent with it being SnO_2.

We apply the same analysis to the pure tin perovskite $FASnI_3$ (Figure 2b and Table 1). In N_2, the TGA curves are characterized by two reasonably distinct mass losses: the first due to sublimation of the organic cation and the second due to evaporation of the metal halide at elevated temperatures, as has been previously observed for pure lead perovskites.[18] Just as with SnI_2, the mass loss in air occurs at much lower temperatures (100−200 °C) than in N_2. In cases where we observe two distinct mass loss regimes, we define the mass remaining after the first regime to be the mass at which there is a strong reduction in slope, determined from the derivatives of the mass versus temperature curves, as described in the experimental section (Supporting Information). In air we also observe two distinct mass loss regimes, which we assign to oxidation followed by FAI evaporation. The final mass of 14.8% is so low that it requires loss of Sn species (rather than just FA and I species) via sublimation of SnI_4 as described in reaction scheme 3a,b. Some of the organic cation will be subliming even at lower temperatures, explaining the higher than predicted mass loss for the first part of the TGA profile. The oxidation reaction mechanism for pure Sn perovskites is then analogous to that of SnI_2 and can thus be summarized by the following reaction scheme I:

$$2ASnI_3 + O_2 \rightarrow 2AI + SnO_2 + SnI_4 \quad (I)$$

where A denotes A site cations such as MA or FA. The oxidation mechanism involving I_2 gas formation and evolution (4a,b) is apparently less favored than that in which SnI_4 is released in these compounds (3a,b). This may be because reaction scheme 4a,b requires all six Sn−I bonds to be broken

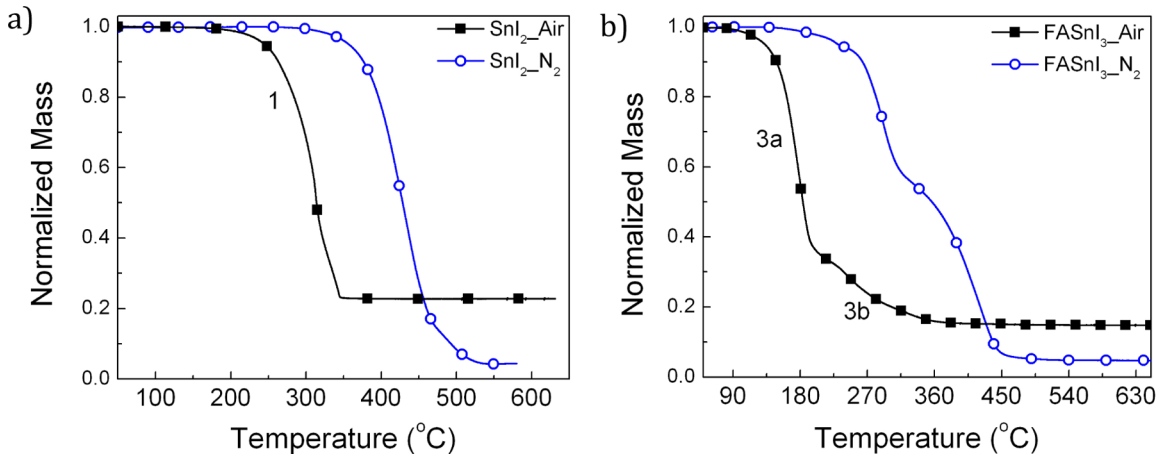

Figure 2. Thermogravimetric analysis of SnI_2 (a) and $FASnI_3$ (b) powders in air and N_2. Markers are just for ease of viewing. The two-step oxidation mechanism for $FASnI_3$ is depicted by labeling the two steps with the most likely scheme as described in Table 1.

DOI: 10.1021/acsenergylett.7b00636
ACS Energy Lett. 2017, 2, 2159−2165

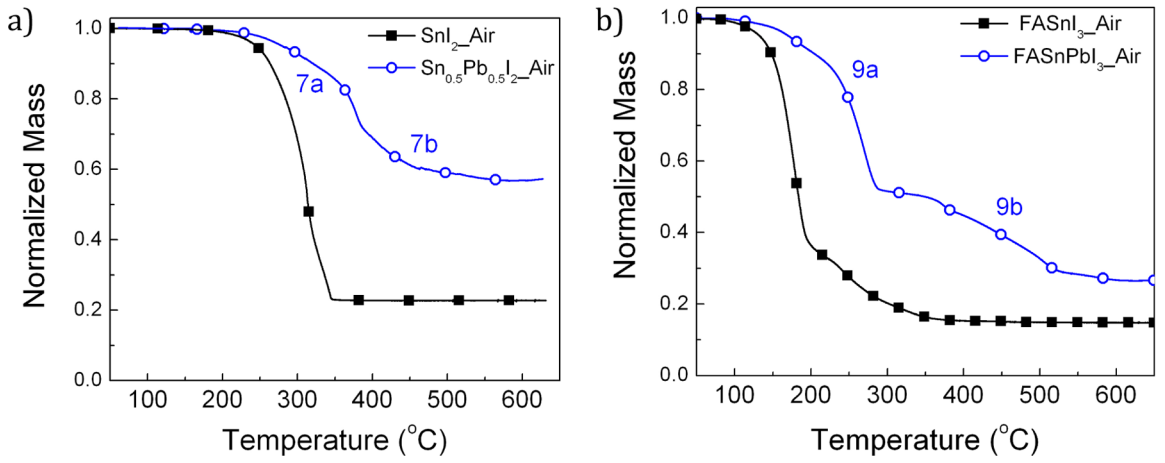

Figure 3. Thermogravimetric analysis of (a) SnI_2 and $SnPbI_4$ powders in air and (b) $FASnI_3$ and $FASn_{0.5}Pb_{.5}I_3$ powders in air. The two-step oxidation mechanisms for $Sn_{0.5}Pb_{0.5}I_2$ and $FASn_{0.5}Pb_{0.5}I_3$ are depicted by labeling the two steps with the most likely schemes as described in Table 2.

Table 2. Possible Steps in Oxidation Mechanisms and Associated Predicted Mass Losses[a]

	Mass loss(%)	Final Mass(%)
$SnPbI_4$		
(5) $2PbSnI_4 + O_2 \Rightarrow 2SnI_4 + 2PbO$	73.2	26.8
(6a) $2PbSnI_4 + O_2 \Rightarrow SnI_4 + SnO_2 + 2PbI_2$	35.6	64.4
(6b) $+ O_2 \Rightarrow SnI_4 + SnO_2 + 2PbO + 2I_2$	64.2	35.8
(7a) $PbSnI_4 + O_2 \Rightarrow SnO_2 + PbI_2 + I_2$	*26.5*	*73.5*
(7b) $+ O \Rightarrow 2SnO_2 + 2PbO_2 + 4I_2$	*55.1*	*44.9*
Measured (±2, ±0.1)	**28, 43.4**	**72, 56.6**
$FASn_{0.5}Pb_{0.5}I_3$		
(8a) $4FAPb_{0.5}Sn_{0.5}I_3 + O_2 \Rightarrow 4FAI(g)+SnI_4(g) + SnO_2 + 2PbI_2$	54.4	45.6
(8b) $+O_2 \Rightarrow 4FAI(g)+SnI_4(g) + SnO_2 + 2PbO + 2I_2(g)$	74.6	25.4
(9a) $4FAPb_{0.5}Sn_{0.5}I_3 + O_2 \Rightarrow 2FAI(g) + SnO_2 + PbI_2 + I_2(g)$	*48.0*	*52.0*
(9b) $+O_2 \Rightarrow 2FAI(g) + SnO_2 + 2PbO + 2I_2(g)$	*68.2*	*31.8*
Measured (±1, ±0.1)	**48, 73.3**	**52, 26.7**

[a]The mechanisms in blue are those that are most likely based on agreement with our experimental data (bold). The experimental data is tabulated as mass losses associated with the first and second steps. $PbSnI_4$ is equivalent to $Pb_{0.5}Sn_{0.5}I_2$, but we use this nomenclature here for ease of displaying the reaction mechanisms.

rather than just two (per $2FASnI_3$), which could raise the activation energy.

We also performed TGA on $Sn_{0.5}Pb_{0.5}I_2$ and $FASn_{0.5}Pb_{0.5}I_3$ in air (Figure 3a,b), and the results reveal that the lead-containing compounds oxidize via a different pathway. The lead-containing compounds oxidize at substantially higher temperatures than the pure tin compounds (~300 and 200 °C vs ~250 and 150 °C for the metal halide and perovskite powders respectively), consistent with our observations during in situ XRD measurements. We present the most probable oxidation reaction schemes in Table 2. We predict that the first step corresponds to oxidation and corresponding evolution of the relatively volatile iodine containing species (SnI_4 or I_2) and FAI (in the case of $FASn_{0.5}Pb_{.5}I_3$), while the second step is likely a convolution of oxidation (to various lead oxide species) and evaporation of the remaining PbI_2 (see Figure S6 for TGA of PbI_2 in air). Focusing on the mass lost in the first part of the TGA decays allows us to elucidate whether SnI_4 is evolved as is the case for $FASnI_3$, or whether the degradation occurs via an altered pathway. Table 2 shows that the mass losses in the first part of the reaction (for both the metal halide and the perovskite compounds) are too low to involve the evolution of SnI_4 but line up nicely with those expected for the formation of SnO_2, PbI_2, and evolution of I_2 (reactions 7a and 9a for the metal halide and the perovskite compounds respectively). This is especially clear in the case of $FASn_{0.5}Pb_{0.5}I_3$, where the two mass loss regimes are separated by >50 °C of fairly constant mass. We thus find that substituting some tin for lead results in increased resistance to oxidation and that the oxidation occurs via a different route. SnI_4 formation is apparently prevented by alloying Sn and Pb, forcing the oxidation reaction to proceed through the less favorable pathway, requiring more Sn−I and Pb−I bonds to break to form I_2 instead (reaction scheme II). Indeed, we find (Figure S8) that the activation energy for this

DOI: 10.1021/acsenergylett.7b00636
ACS Energy Lett. 2017, 2, 2159−2165

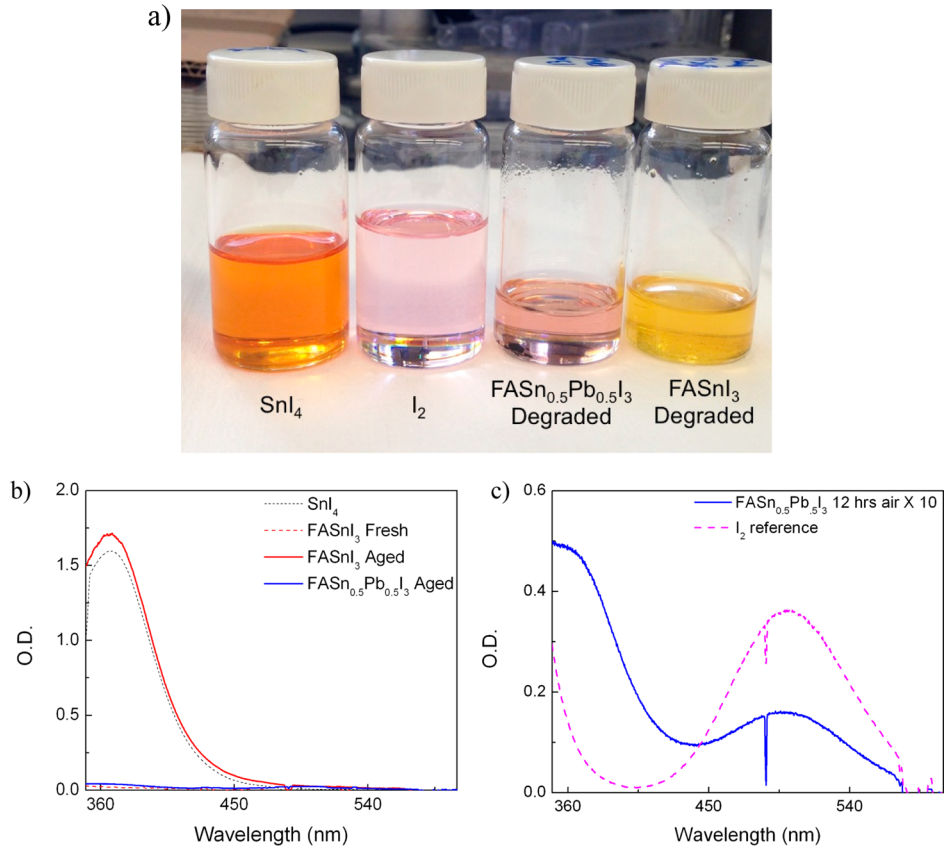

Figure 4. (a) Photographs of SnI_4, I_2, degraded $FASn_{0.5}Pb_{0.5}I_3$, and degraded $FASnI_3$ powders immersed in benzene. The perovskite powders were degraded by heating at 70 °C for 12 h on a hot plate in air. They were then immersed in benzene so that the degradation products could leach into solution. The absorption spectra of the resultant solutions are provided in panel b at 0.2 mM concentration and in panel c at 2.4 mM. SnI_4 (0.14 mM) and I_2 (0.74 mM) reference spectra are provided in panels b and c, respectively. The cuvette was 1 cm wide.

process is higher (731 meV) than that for scheme I for the pure tin perovskites (537 meV), supporting the idea that more energy is required to initiate reaction II than I, perhaps because more Sn−I bonds must be broken.

$$2ASn_{0.5}Pb_{0.5}I_3 + O_2 \rightarrow 2AI + SnO_2 + PbI_2 + I_2 \qquad (II)$$

The TGA data allows us to evaluate the degradation mechanism at high temperatures. At lower temperatures, we expect the same oxidation pathway to occur but would not expect the products to evolve as gases, allowing us to directly detect their presence. The SnI_4 and I_2 products have distinct absorption spectra, so we can use them as markers to directly validate our proposed reaction schemes I and II. Here, we simply degrade $FASnI_3$ and $FASn_{0.5}Pb_{0.5}I_3$ powders by heating them at 70 °C in air for 12 h. This ensures degradation but prevents the products from evaporating. We disperse the degraded powders in benzene, in which the perovskites and precursors are insoluble but the SnI_4 and I_2 degradation products are highly soluble. The photo in Figure 4a compares SnI_4 and I_2 references to degraded $FASnI_3$ and $FASn_{0.5}Pb_{0.5}I_3$ powders in benzene. The degraded $FASnI_3$ sample exhibits the same yellow-orange color as the SnI_4 reference solution, while the degraded $FASn_{0.5}Pb_{0.5}I_3$ exhibits the same pink-purple color as the I_2 reference solution. UV−vis absorption spectra of the different solutions are plotted in Figures 4b,c, and we confirm that the main degradation product of the $FaSnI_3$ compound is SnI_4, while that of the lead-containing compound is I_2. There does, however, appear to be a yellow tint and increased absorption in the low-wavelength part of the spectrum for the degraded $FASn_{0.5}Pb_{0.5}I_3$ powder. Using extinction coefficients of the products in benzene (Figure S9) we confirm that there is only a minimal (20× less than for $FASnI_3$, and 10× less than I_2) amount of SnI_4 in the oxidized $FASn_{0.5}Pb_{.5}I_3$, confirming that the predominant degradation mechanism produces I_2 rather than SnI_4 for lead-containing compounds. This method for detecting the presence of the reaction products proved very powerful, allowing us to detect and distinguish between amorphous products of similar compositions.

Our analysis of XRD, TGA, and absorption spectroscopy demonstrates that incorporating lead into tin halide and tin halide perovskite compounds dramatically slows the oxidation and forces it to proceed via a different mechanism, one where all the S−I bonds are broken and where the main iodine-containing product is I_2 rather than SnI_4. We propose that this alternate oxidation mechanism is precisely what allows lead to stabilize tin-based perovskites. The formation of SnI_4 species along with SnO_2 is most likely to involve the cooperative action of several tin iodide octahedra, where the iodide ions bonded to one tin cation can be transferred onto adjacent tin cations with which the iodide was shared. Lead, however, cannot be easily oxidized to a Pb^{4+} and is unlikely to form PbI_4. Hence, if many of the B sites are occupied by lead rather than tin, then the cooperative mechanism is far less favorable. Instead, I_2 is formed, and this requires three times as many Sn−I bonds to be broken. In the Supporting Information (Figure S10) we show that the likelihood of finding multiple adjacent tin cations drops very steeply with increasing lead content and does so in a similar way to the oxidation lifetimes plotted in Figure 1b. We

DOI: 10.1021/acsenergylett.7b00636
ACS Energy Lett. 2017, 2, 2159−2165

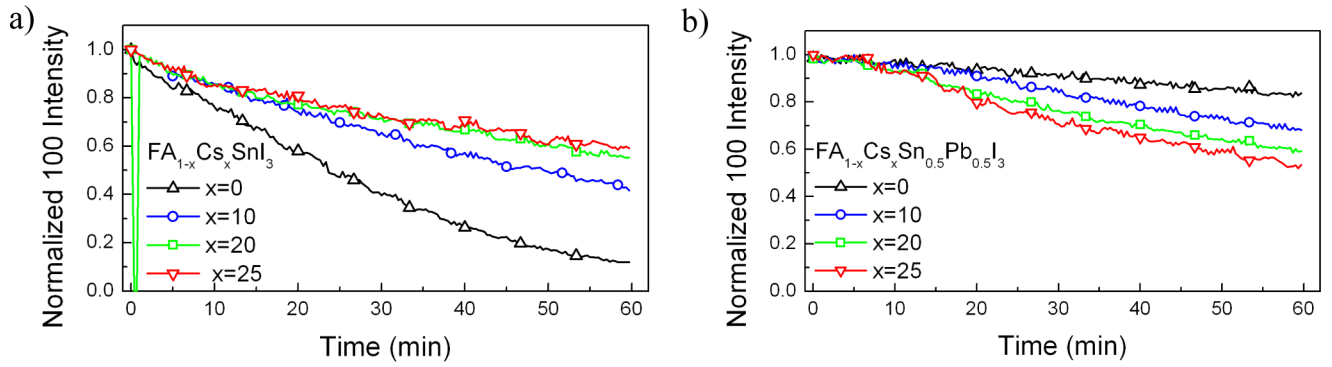

Figure 5. Normalized 100 peak heights are monitored by XRD for $FA_{1-x}Cs_xSnI_3$ (a) and $FA_{1-x}Cs_xSn_{0.5}Pb_{0.5}I_3$ (b) in dry air at 85 °C.

hypothesize the cooperative oxidation of many adjacent tin iodide octahedra can be prevented by incorporating stable 2+ metal cations that will not readily oxidize to 4+ states. Lead is not the only such metal, so we believe that this hypothesis may lead to new developments in stabilizing tin-based perovskites by tuning of the B site composition.

Because most of the state-of-the-art perovskite solar cells are made with compositions incorporating multiple A site cations, we also investigate the influence of the A site composition on the stability of tin-based perovskites. We previously replaced some of the FA on the A site with Cs to make efficient $FA_{0.75}Cs_{0.25}Sn_{0.5}Pb_{0.5}I_3$ solar cells. Here, we again employ XRD and monitored the (100) peak intensity as a function of time at 85 °C in dry air for $FA_{1-x}Cs_xSnI_3$ and $FA_{1-x}Cs_xSn_{0.5}Pb\ I_3$. The results are plotted in Figure 5. We observe a surprising trend: the pure tin compounds are stabilized by Cs substitution while the tin−lead compounds exhibit reduced stability upon Cs substitution. The peak positions, plotted in Figure S11, show a general reduction in lattice parameter for all the Cs-containing compounds as they oxidize, indicating that the materials are being enriched in cesium. We propose that reducing the cubic lattice parameter in the $FA_{1-x}Cs_xSnI_3$ series shortens and strengthens the Sn−I bond. The mixed Sn:Pb compounds, however, are losing Sn cations to oxidation, as indicated by the rising lattice parameter for the cesium free $FASn_{0.5}Pb_{0.5}I_3$ (Figures S11 and S12). Hence, we propose that the Sn:Pb perovskites are being enriched in cesium and lead during oxidation, and we find that this causes phase instability and even some phase segregation (Figure S12) of cesium-rich compositions, as evidenced by broadening of the XRD peak width and the appearance of a broad shoulder corresponding to phases with a small lattice parameter. Li et al.[19] previously demonstrated that compounds that are rich in cesium and lead do not form stable perovskite phases at moderate temperatures, so we propose that increased phase instability is contributing to the rapid degradation in the cesium containing Sn:Pb perovskites. This is validated by the observation that at higher temperatures (150 °C, Figure S13) in which the cesium- and lead-rich compounds form stable perovskite phases,[19] $FA_{0.8}Cs_{.2}Sn_{.5}Pb_{0.5}I_3$ is actually as stable or even more stable to oxidation than $FaSn_{0.5}Pb_{0.5}I_3$.

The findings presented here provide guidelines for the compositional engineering of tin-based perovskites with enhanced stability. It is essential to minimize the probability of there being networks of adjacent tin-iodide octahedra by using ∼50% or more Pb-substitution, with degradation lifetimes improving by orders of magnitude when only 25% tin is used. It also appears that shrinking the cubic lattice by incorporation of smaller A site cations such as Cs can slow the oxidation reaction. However, when incorporating a smaller cation on to the A site, it is essential for this cation be able to form structurally stable tin and lead perovskite compounds in its own right, to minimize the chances of any additional structural instability arising during oxidation. Future work could explore the impact of other B site substitution to simultaneously shrink the lattice parameter and also replace Sn^{2+} ions. It is likely, however, that solar cells containing any tin at all will require thorough encapsulation; thus, further research should be directed at developing or adapting existing encapsulation strategies. Addressing oxidation in Sn-based perovskites will be key, and developing our understanding of the oxidation mechanisms provides a first step toward viable all-perovskite tandem solar cells.

■ ASSOCIATED CONTENT

Supporting Information

The Supporting Information is available free of charge on the ACS Publications website at DOI: 10.1021/acsenergylett.7b00636.

Experimental methods, XRD spectra, additional TGA data, simulations, extinction coefficient calculations, XRD peak and positions as a function of time for Cs content series, and activation energy calculation (PDF)

■ AUTHOR INFORMATION

Corresponding Authors

*E-mail: mmcgehee@stanford.edu.

*E-mail: toleijtens@gmail.com.

ORCID

Tomas Leijtens: 0000-0001-9313-7281

Rohit Prasanna: 0000-0002-9741-2348

Michael F. Toney: 0000-0002-7513-1166

Michael D. McGehee: 0000-0001-9609-9030

Author Contributions

‖T.L. and R.P. contributed equally to this work.

Notes

The authors declare no competing financial interest.

■ ACKNOWLEDGMENTS

T.L. is funded by a Marie Sklodowska Curie International Fellowship under Grant Agreement H2O2IF-GA-2015-659225. We also acknowledge the Office of Naval Research USA for support. Use of the Stanford Synchrotron Radiation Lightsource, SLAC National Accelerator Laboratory, is supported by

DOI: 10.1021/acsenergylett.7b00636
ACS Energy Lett. 2017, 2, 2159−2165

the U.S. Department of Energy, Office of Science, Office of Basic Energy Sciences under Contract No. DE-AC02-76SF00515. We thank Dr. Giles Eperon for valuable discussions. Part of this work was performed at the Stanford Nano Shared Facilities (SNSF), supported by the National Science Foundation under award ECCS-1542152.

REFERENCES

(1) Eperon, G. E.; Leijtens, T.; Bush, K. A.; Prasanna, R.; Green, T.; Wang, J. T.-W.; McMeekin, D. P.; Volonakis, G.; Milot, R. L.; May, R. Perovskite-Perovskite Tandem Photovoltaics with Optimized Bandgaps. *Science (Washington, DC, U. S.)* **2016**, *354*, 861.

(2) Zhao, D.; Yu, Y.; Wang, C.; Liao, W.; Shrestha, N.; Grice, C. R.; Cimaroli, A. J.; Guan, L.; Ellingson, R. J.; Zhu, K.; et al. Low-Bandgap Mixed Tin−lead Iodide Perovskite Absorbers with Long Carrier Lifetimes for All-Perovskite Tandem Solar Cells. *Nat. Energy* **2017**, *2*, 17018.

(3) Liao, W.; Zhao, D.; Yu, Y.; Shrestha, N.; Ghimire, K.; Grice, C. R.; Wang, C.; Xiao, Y.; Cimaroli, A. J.; Ellingson, R. J.; et al. Fabrication of Efficient Low-Bandgap Perovskite Solar Cells by Combining Formamidinium Tin Iodide with Methylammonium Lead Iodide. *J. Am. Chem. Soc.* **2016**, *138*, 12360−12363.

(4) Forgács, D.; Gil-Escrig, L.; Pérez-Del-Rey, D.; Momblona, C.; Werner, J.; Niesen, B.; Ballif, C.; Sessolo, M.; Bolink, H. J. Efficient Monolithic Perovskite/Perovskite Tandem Solar Cells. *Adv. Energy Mater.* **2017**, *7*, 1602121.

(5) Yang, Z.; Rajagopal, A.; Chueh, C. C.; Jo, S. B.; Liu, B.; Zhao, T.; Jen, A. K. Y. Stable Low-Bandgap Pb−Sn Binary Perovskites for Tandem Solar Cells. *Adv. Mater.* **2016**, *28*, 8990−8997.

(6) Hao, F.; Stoumpos, C. C.; Chang, R. P. H.; Kanatzidis, M. G. Anomalous Band Gap Behavior in Mixed Sn and Pb Perovskites Enables Broadening of Absorption Spectrum in Solar Cells. *J. Am. Chem. Soc.* **2014**, *136*, 8094−8099.

(7) Rajagopal, A.; Yang, Z.; Jo, S. B.; Braly, I. L.; Liang, P.; Hillhouse, H. W.; Jen, A. K. Highly Efficient Perovskite−Perovskite Tandem Solar Cells Reaching 80% of the Theoretical Limit in Photovoltage. *Adv. Mater.* **2017**, 1702140.

(8) Hoshi, H.; Shigeeda, N.; Dai, T. Improved Oxidation Stability of Tin Iodide Cubic Perovskite Treated by 5-Ammonium Valeric Acid Iodide. *Mater. Lett.* **2016**, *183*, 391−393.

(9) Noel, N. K.; Stranks, S. D.; Abate, A.; Wehrenfennig, C.; Guarnera, S.; Haghighirad, A.-A.; Sadhanala, A.; Eperon, G. E.; Pathak, S. K.; Johnston, M. B.; et al. Lead-Free Organic-Inorganic Tin Halide Perovskites for Photovoltaic Applications. *Energy Environ. Sci.* **2014**, *7*, 3061−3068.

(10) Marshall, K. P.; Walker, M.; Walton, R. I.; Hatton, R. A. Enhanced Stability and Efficiency in Hole-Transport-Layer-Free CsSnI3 Perovskite Photovoltaics. *Nat. Energy* **2016**, *1*, 16178.

(11) Marshall, K. P.; Walton, R. I.; Hatton, R. A. Tin Perovskite/fullerene Planar Layer Photovoltaics: Improving the Efficiency and Stability of Lead-Free Devices. *J. Mater. Chem. A* **2015**, *3*, 11631−11640.

(12) Hao, F.; Stoumpos, C. C.; Cao, D. H.; Chang, R. P. H.; Kanatzidis, M. G. Lead-Free Solid-State Organic-Inorganic Halide Perovskite Solar Cells. *Nat. Photonics* **2014**, *8*, 489−494.

(13) Lee, S. J.; Shin, S. S.; Kim, Y. C.; Kim, D.; Ahn, T. K.; Noh, J. H.; Seo, J.; Seok, S. Il. Fabrication of Efficient Formamidinium Tin Iodide Perovskite Solar Cells through SnF2-Pyrazine Complex. *J. Am. Chem. Soc.* **2016**, *138*, 3974−3977.

(14) Kostko, V. S.; Kostko, O. V.; Makovetskii, G. I.; Yanushkevich, K. I. Thin Film Structure of tin(II) Iodide. *Phys. Status Solidi B* **2002**, *229*, 1349−1352.

(15) Sawada, Y.; Suzuki, M. Thermal Change of SnI2 Thin Films: Part 1. Thermogravimetry. *Thermochim. Acta* **1994**, *232*, 29−36.

(16) Sawada, Y.; Suzuki, M. Thermal Change of SnI2 Thin Films. Part 3. Isothermal Change under Light Radiation. *Thermochim. Acta* **1994**, *243*, 95−100.

(17) Sawada, Y.; Suzuki, M. Thermal Change of SnI2 Thin Films. Part 4. TG-DTA and DSC. *Thermochim. Acta* **1995**, *254*, 261−266.

(18) Dualeh, A.; Gao, P.; Seok, S. Il; Nazeeruddin, M. K.; Gratzel, M. Thermal Behavior of Methylammonium Lead-Trihalide Perovskite Photovoltaic Light Harvesters. *Chem. Mater.* **2014**, *26*, 6160−6164.

(19) Li, Z.; Yang, M.; Park, J.-S.; Wei, S.-H.; Berry, J. J.; Zhu, K. Stabilizing Perovskite Structures by Tuning Tolerance Factor: Formation of Formamidinium and Cesium Lead Iodide Solid-State Alloys. *Chem. Mater.* **2016**, *28*, 284−292.

DOI: 10.1021/acsenergylett.7b00636
ACS Energy Lett. 2017, 2, 2159−2165